

See discussions, stats, and author profiles for this publication at: <https://www.researchgate.net/publication/263713071>

Synthesis and Biological Evaluation of F-18-Labeled Fluoroethoxy Tryptophan Analogues as Potential PET Tumor Imaging Agents

ARTICLE in MOLECULAR PHARMACEUTICS · JULY 2014

Impact Factor: 4.38 · DOI: 10.1021/mp500312t · Source: PubMed

CITATIONS

3

READS

66

7 AUTHORS, INCLUDING:



Adrienne Müller Herde

ETH Zurich

46 PUBLICATIONS 754 CITATIONS

[SEE PROFILE](#)



Lijing Mu

University of Zurich

52 PUBLICATIONS 744 CITATIONS

[SEE PROFILE](#)



Stefanie D Krämer

ETH Zurich

100 PUBLICATIONS 1,609 CITATIONS

[SEE PROFILE](#)



Simon Ametamey

ETH Zurich

176 PUBLICATIONS 3,108 CITATIONS

[SEE PROFILE](#)

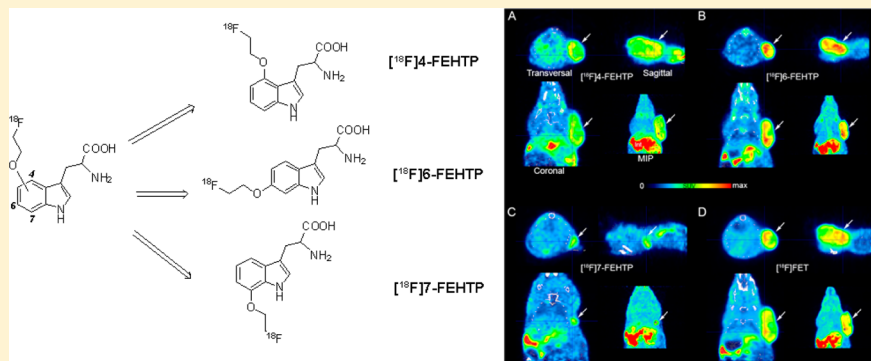
Synthesis and Biological Evaluation of ^{18}F -Labeled Fluoroethoxy Tryptophan Analogs as Potential PET Tumor Imaging Agents

Aristeidis Chiotellis,[†] Adrienne Muller,[†] Linjing Mu,[‡] Claudia Keller,[†] Roger Schibli,^{†,‡}
Stefanie D. Krämer,[†] and Simon M. Ametamey^{*,†}

[†]Center for Radiopharmaceutical Sciences ETH-PSI-USZ, Institute of Pharmaceutical Sciences ETH, Vladimir-Prelog-Weg 4, 8093 Zurich, Switzerland

[‡]Center for Radiopharmaceutical Sciences ETH-PSI-USZ, Department of Nuclear Medicine, University Hospital Zurich, Rämistrasse 100, 8091 Zurich, Switzerland

Supporting Information



ABSTRACT: As a continuation of our research efforts toward the development of tryptophan-based radiotracers for tumor imaging with positron emission tomography (PET), three new fluoroethoxy tryptophan analogues were synthesized and evaluated *in vivo*. These new tracers (namely, 4-(2-[^{18}F]fluoroethoxy)-DL-tryptophan ($[^{18}\text{F}]4\text{-FEHTP}$), 6-(2-[^{18}F]fluoroethoxy)-DL-tryptophan ($[^{18}\text{F}]6\text{-FEHTP}$), and 7-(2-[^{18}F]fluoroethoxy)-DL-tryptophan ($[^{18}\text{F}]7\text{-FEHTP}$) carry the fluoroethoxy side chain either at positions 4-, 6-, or 7- of the indole core. Reference compounds and precursors were synthesized by multistep approaches. Radiosynthesis was accomplished by no-carrier-added nucleophilic ^{18}F -fluorination following either an indirect approach (O-alkylation of the corresponding hydroxytryptophan with [^{18}F]fluoroethyltosylate) or a direct approach (nucleophilic ^{18}F fluorination using a protected mesyl precursor). Radiochemical yields (decay corrected) for both methods were in the range of 10–18%. Small animal PET imaging with xenograft-bearing mice revealed the highest tumor/background ratio for $[^{18}\text{F}]6\text{-FEHTP}$ which, in a direct comparison, outperformed the other two tryptophan tracers and also the well-established tyrosine analogue *O*-(2-[^{18}F]fluoroethyl)-L-tyrosine ($[^{18}\text{F}]1\text{-FET}$). Investigation of the transport mechanism of $[^{18}\text{F}]6\text{-FEHTP}$ in small cell lung cancer cells (NCI-H69) revealed that it is most probably taken up exclusively via the large neutral amino acid transporter(s) (LAT).

KEYWORDS: tryptophan, tumor imaging, PET, LAT1

INTRODUCTION

Positron emission tomography (PET) allows the functional evaluation of metabolic irregularities associated with several hallmarks of cancer,¹ which provides an opportunity to delineate normal and tumor tissue on the basis of functional PET imaging.² The rapid growth and continuous proliferation of cancer cells demand a high rate of protein synthesis, which is satisfied by an increased uptake of amino acids to be used either as energy source or as building blocks for various biosyntheses.³ This has fueled many efforts toward the labeling of numerous amino acids with PET radionuclides (mainly ^{11}C and ^{18}F), turning them into a promising class of tracers,⁴ which in some cases, seem to be advantageous over the most successful tumor PET agent 2-[^{18}F]fluoro-2-deoxy-D-glucose ($[^{18}\text{F}]FDG$).^{5,6}

The transfer of amino acids across plasma membranes is mediated through specialized transporters, and more than 20 distinct carrier proteins have been identified in mammalian cells differing in terms of substrate specificity, transport mechanism, and functionality. These amino acid transport systems are mainly categorized in four families, designated as systems L (leucine preferring), A (alanine preferring), ASCT (alanine,

Special Issue: Positron Emission Tomography: State of the Art

Received: April 28, 2014

Revised: June 30, 2014

Accepted: July 2, 2014

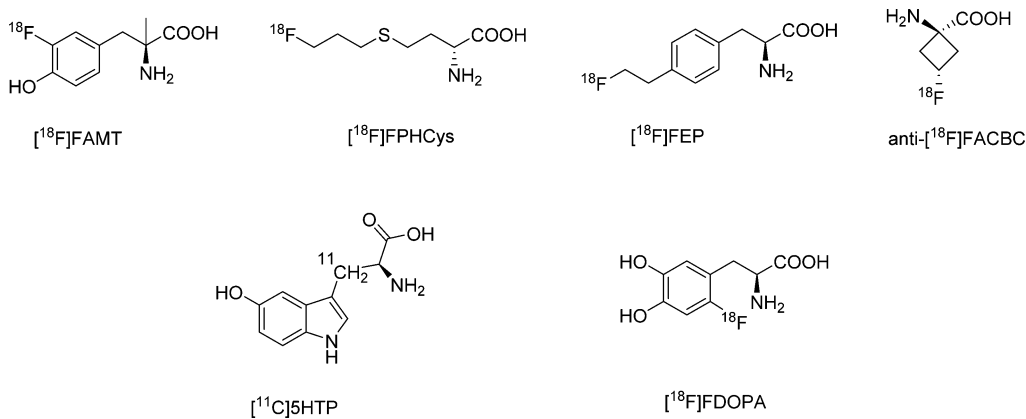


Figure 1. Structures of some amino acid tumor imaging agents for PET. The uptake of these tracers is mainly via LAT1. [¹¹C]5HTP and [¹⁸F]FDOPA are additionally decarboxylated in vivo.

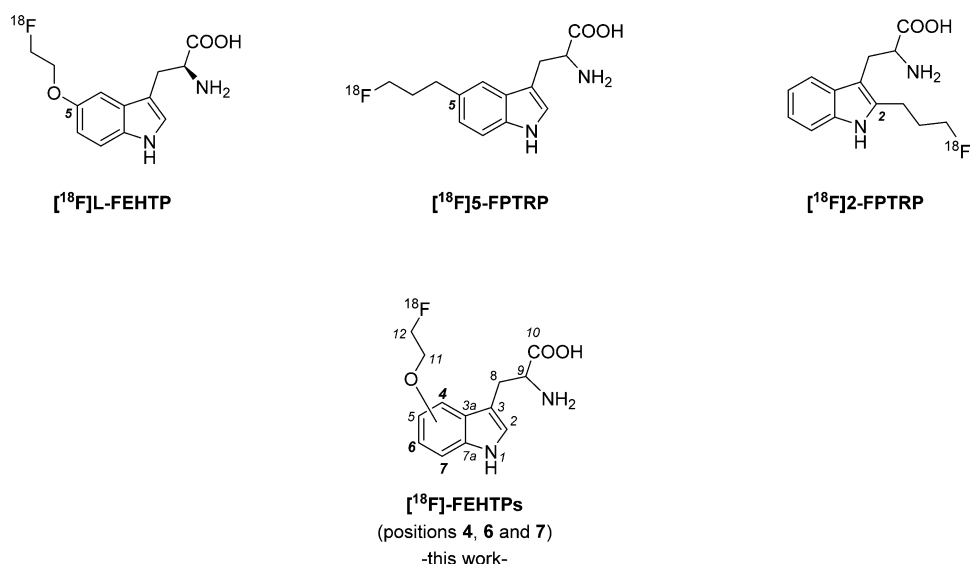


Figure 2. Chemical structures of [¹⁸F]-l-FEHTP, [¹⁸F]-5-FPTRP, [¹⁸F]-2-FPTRP and of the new fluoroethoxy tryptophan derivatives. The numbering of the atoms of the tryptophan core and side chain is shown to facilitate NMR characterization.

serine, cysteine transport), and cationic transporters.^{4,7,8} In malignant lesions, the high demand of amino acids is satisfied through angiogenesis and upregulation of certain transporters.^{3,7} In particular, increased expression of the system L subtype LAT1 (SLC7A5)/4F2hc (SLC3A2), system ASC subtype ASCT2 (SLC1A5), and sodium- and chloride-dependent neutral and basic amino acid transporter B⁰⁺ (ATB^{0+,+}, SLC6A14) have been associated with cell proliferation and cancer growth.^{9–12}

Over the past decade, LAT1 has been the center of scientific interest because it was found that a wide range of tumor cell lines, primary human cancers, and metastases show marked expression of this transporter. LAT1 is a Na⁺-independent large neutral amino acid transporter which requires an additional protein, the heavy chain of the 4F2 antigen which forms a heterodimeric functional complex with the LAT1 protein.¹³ Upregulation of LAT1 correlates with cell proliferation and angiogenesis, and it has been observed in cancers of brain, colon, lung, liver, and skin,³ whereas it was a significant prognostic factor for predicting poor outcome in certain malignancies.¹⁴ LAT1 is considered to be oncogenic because inhibition of system L transport activity by 2-aminobicyclo-(2,2,1)-heptane-2-carboxylic acid (BCH) induces apoptosis in

some cancer lines.¹⁴ Recently, it was also shown that LAT1 seems to regulate multiple cellular activities including tumor cell proliferation through the mammalian target of rapamycin pathway (mTOR).¹⁵ Thus, LAT1 is considered to be both a prognosis marker and a therapeutic target in cancer, which encouraged efforts toward the development of PET tracers targeting specifically this transporter. A number of radiolabeled amino acids (Figure 1) including derivatives of tyrosine (L-[3-¹⁸F]- α -methyltyrosine, [¹⁸F]FAMT),¹⁶ methionine (S-(3-¹⁸F)fluoropropyl)-D-homocysteine, [¹⁸F]FPHCys),¹⁷ phenylalanine (L-p-(2-¹⁸F)fluoroethyl)phenylalanine, [¹⁸F]FEP),¹⁸ and leucine (anti-1-amino-3-[¹⁸F]-fluorocyclobutane-1-carboxylic acid ([¹⁸F]FACBC)¹⁹ have been shown to mainly target LAT1 activity.

Recently, three derivatives of tryptophan, namely, (5-(2-¹⁸F)fluoroethoxy)-L-tryptophan ([¹⁸F]L-FEHTP),²⁰ 2-(3-¹⁸F)fluoropropyl)-DL-tryptophan ([¹⁸F]2-FPTRP), and 5-(3-¹⁸F)fluoro-propyl)-DL-tryptophan ([¹⁸F]5-FPTRP)²¹ (Figure 2) were developed in our lab and characterized pharmacologically. Results showed that the new tracers are promising PET probes for the LAT activity of malignant lesions. Although the amino acid tryptophan is a fairly good (albeit not the best) substrate for the aromatic amino acid decarboxylase (AADC),²²

the new tryptophan analogues seem to abolish this feature, because only the intact compound was detected in plasma for all tracers up to 60 min post injection (p.i.). Amino acid tracers that are substrates for AADC are advantageous for endocrine tumor imaging^{23,24} because these slowly growing malignant lesions, which are not easily detected with [¹⁸F]FDG, show enhanced expression of this enzyme.²⁵ In vivo decarboxylation of these amino acids by AADC converts them to biogenic amines which can be stored in secretory vesicles, a mechanism which leads to their trapping inside the cancer cell (APUD concept, Amine Precursor Uptake and Decarboxylation).²⁶ Two amino acid tracers that exhibit this characteristic are L-3,4-dihydroxy-6-[¹⁸F]fluorophenylalanine ([¹⁸F]FDOPA)²⁷ and 5-hydroxy-L-[β -¹¹C]tryptophan ([¹¹C]SHTP) (Figure 2).²⁸

Despite the fact that our new tryptophan-based tracers were not substrates for AADC, their good in vivo tumor accumulation encouraged us to investigate further analogues of tryptophan as potential tumor PET probes. We chose to develop structural analogues of [¹⁸F]L-FEHTP where the 2-fluoroethoxy side chain is situated at different positions on the indole ring, namely, positions 4-, 6- and 7-. The different localization of the fluorine-bearing side chain on the indole core is expected to have effects on the electronic properties of the new analogues compared to [¹⁸F]L-FEHTP. This could potentially lead to tracers with improved in vivo pharmacokinetics resulting in higher tumor uptake or enhanced tumor/background ratios. In this respect, we were interested in verifying how this structural modification would alter the in vivo behavior of the new analogues, hoping for tracers that are better substrates for LAT or even substrates of the enzyme AADC.

In this work, we describe the synthesis, radiolabeling, and biological evaluation of three new tryptophan derivatives, (4-(2-[¹⁸F]fluoroethoxy)-DL-tryptophan ([¹⁸F]4-FEHTP), (6-(2-[¹⁸F]fluoroethoxy)-DL-tryptophan ([¹⁸F]6-FEHTP) and (7-(2-[¹⁸F]fluoroethoxy)-DL-tryptophan ([¹⁸F]7-FEHTP) (Figure 2) and their comparison with [¹⁸F]L-FET, the most commonly used amino acid PET tracer in the clinic and our previous analogue, [¹⁸F]L-FEHTP. For the in vitro and in vivo evaluations, we chose the endocrine small cell lung cancer cell line NCI-H69, which shows enhanced expression of LAT1 levels²⁹ and displays high AADC activity.³⁰

EXPERIMENTAL SECTION

Materials and Methods. All reagents were purchased from commercial suppliers and used without further purification. Starting materials **1** (4-benzyloxy-NBoc tryptophan), **12** (6-benzyloxy-NFmoc tryptophan), and **23** (7-hydroxytryptophan) were obtained from Rare Chemicals GmbH, HDH Pharma Inc. and SynChem UG & Co., respectively. 2-Fluoroethyl 4-methylbenzenesulfonate³¹ and 2-((*tert*-butyldimethylsilyl)oxy)-ethyl 4-methylbenzenesulfonate^{32,33} were synthesized from 2-fluoroethanol and ethylene glycol, respectively, by following published protocols with some modifications. All solvents used for reactions were purchased as anhydrous grade from Acros Organics (puriss., dried over molecular sieves, H₂O < 0.005%) and were used without further purification unless otherwise stated. Solvents for extractions, column chromatography, and thin-layer chromatography (TLC) were purchased as commercial grade. All nonaqueous reactions were performed under an argon atmosphere using flame-dried glassware and standard syringe/septa techniques. In general, reactions were magnetically stirred and monitored by TLC performed on Merck TLC

glass sheets (silica gel 60 F₂₅₄). Spots were visualized with UV light ($\lambda = 254$ nm) or through staining with anisaldehyde solution or basic aq KMnO₄ solution and subsequent heating. Chromatographic purification of products was performed using Fluka silica gel 60 for preparative column chromatography (particle size 40–63 μ m). Reactions at 0 °C were carried out in an ice/water bath. Nuclear magnetic resonance (NMR) spectra were recorded in CDCl₃, CD₃OD, or DMSO-*d*₆ on a Bruker Av-400 spectrometer at room temperature. The measured chemical shifts are reported in δ (ppm), and the residual signal of the solvent was used as the internal standard (CDCl₃: ¹H: $\delta = 7.26$ ppm; ¹³C: $\delta = 77.0$ ppm; CD₃OD: ¹H: $\delta = 3.31$ ppm; ¹³C: $\delta = 49.1$ ppm; DMSO-*d*₆: ¹H: $\delta = 2.50$ ppm; ¹³C: $\delta = 39.51$ ppm). For the ¹⁹F NMR spectra, CFCl₃(= 0.00 ppm) was used as the internal standard. All ¹³C NMR spectra were measured with complete proton decoupling. Data of NMR spectra are reported as follows: s = singlet, d = doublet, t = triplet, m = multiplet, dd = doublet of doublets, dt = doublet of triplets, dq = doublet of quartets, br = broad signal. The coupling constant J is reported in Hertz (Hz). The numbering of the H and C atoms can be seen in Figure 2. High-resolution mass spectrometry (HRMS) was performed on a Bruker Daltonics maxis ESI-QTOF or a Varian HiResMALDI instrument.

High-performance liquid chromatography (HPLC) was performed on a Merck-Hitachi L-7000 system equipped with an L-7400 tunable absorption detector. Analytical HPLC was performed with a reverse-phase column (Ultimate XB-C18 4.6 × 150 mm, 3 μ m) with the following solvent systems; **Method A:** water (solvent A), acetonitrile (solvent B); 0–15 min: 30–95% B, 15–23 min: 95% B, 23–25 min: 95–30% B, 25–30 min 30% B; flow 1 mL/min; UV = 280 nm. **Method B:** water (solvent A), acetonitrile (solvent B); 0–30 min 5–70% B; flow 1 mL/min; UV = 280 nm. **Method C:** water (solvent A), acetonitrile (solvent B); 0–5 min: 5% B, 5–25 min: 5–90% B, 25–30 min: 90% B; flow 15 mL/min; UV = 280 nm. Preparative HPLC was performed with a reverse-phase preparative column (Ultimate XB-C18 21.2 × 150 mm, 5 μ m) using the following methods; **Method D:** water (solvent A), acetonitrile (solvent B); 0–30 min: 5–70% B; flow 15 mL/min; UV = 280 nm. **Method E:** water (solvent A), acetonitrile (solvent B); 0–5 min: 5% B, 5–10 min: 5–10% B, 10–20 min: 10–95% B, 20–28 min 95–5% B, 28–30 min: 5% B; flow 15 mL/min; UV = 280 nm

Analytical radio-HPLC was performed on an Agilent 1100 system equipped with multi-UV-wavelength and Raytest Gabi Star detectors and Gina Star software. A reverse phase column was used (LiChrospher 100 RP-18 5 μ m LiChroCART 4 × 250 mm) with the following solvent system: H₂O (0.1% TFA) (solvent A), acetonitrile (solvent B); flow 1 mL/min; 0–3 min: 5% B, 3–15 min: 5–90% B, 15–19 min: 90% B, 19–20 min: 90–5% B, 20–30 min 5% B; UV = 280 nm. Semipreparative purification of radiolabeled material was performed on a Merck-Hitachi L6200A system equipped with Knauer variable wavelength detector and an Emberline radiation detector using a reverse phase column (Phenomenex Luna C18, 10 × 250 mm, 5 μ m) and isocratic conditions consisting of 8% EtOH in 35 mM acetate buffer (pH ≈ 4) at a flow rate of 4 mL/min (UV = 280 nm). For reaction monitoring during radiosynthesis and for the metabolite studies a Waters Ultraprecision liquid chromatography (UPLC) system was used with an Acquity UPLC BEH C18 column (2.1 × 50 mm, 1.7 μ m, Waters) and an attached coincidence detector (FlowStar LBS13, Berthold). The mobile phase consisted of

the following system: H₂O (NH₄HCO₃, 50 mM) (solvent A), acetonitrile (solvent B); flow 0.6 mL/min; 0–0.3 min: 0% B, 0.3–3.3 min: 0–100% B, 3.3–3.8 min: 100% B, 3.8–4.0 min: 100–0% B; UV = 280 nm.

Purity of biologically tested compounds was always ≥95% as determined by the aforementioned analytical radio-HPLC method. Specific activity was calculated by comparing ultraviolet peak intensity of final formulated products with calibration curves of corresponding nonradioactive standards of known concentrations.

Chemistry. General Procedures. Method D (for Mesylation). A solution of mesyl chloride (1.2 equiv) in dichloromethane was added dropwise to an ice-cold solution of **10** or **21** and triethylamine (2.4 equiv) in dichloromethane (0.075 M) and stirring was continued at 0 °C for 1 h while monitoring was performed with HPLC. Subsequently, the reaction was diluted with DCM, washed with NaHCO₃ (sat) (×1), water (×1) and brine (×1), dried over sodium sulfate, filtered, and evaporated to dryness. The crude was purified by preparative HPLC, and the fractions of interest were collected and lyophilized to give the final product.

2-Amino-3-(4-(2-fluoroethoxy)-1*H*-indol-3-yl)propanoic acid (6**), 4-FEHTP.** To an ice-cold suspension of **5** (12 mg, 0.033 mmol) was added TFA (50 μL, 0.66 mmol), and the resulting slight yellow solution was stirred at 0 °C and was allowed to reach room temperature, slowly overnight. Next day, ethyl acetate was added, and the volatiles were removed under reduced pressure. The crude was purified by preparative HPLC following method E (*t*_R ≈ 15 min). Lyophilization of the relevant combined fractions provided **6** as a white solid (4.3 mg, 49%). ¹H NMR (*d*₆-DMSO, 400 MHz) δ: 10.85 (br, 1 H, H-1), 7.01 (d, ³J_{H2–H1} = 2.2 Hz, 1 H, H-2), 6.97–6.94 (m, 2 H, H-6 and H-7), 6.46 (t, 1 H, ³J_{H5–H6} = ³J_{H5–H7} = 4.3 Hz, 1 H, H-5), 4.90 (m, 2 H, H-12), 4.30 (m, 2 H, H-11), 3.62–3.54 (m, 2 H, H-9 and H-8a), 2.82 (dd, ²J_{H8b–H8a} = 15.7 Hz, ³J_{H8b–H9} = 11.3 Hz, 1 H, H-8b). ¹³C NMR (*d*₆-DMSO, 100 MHz) δ: 170.0, 153.2, 136.9, 122.5, 119.9, 118.9, 109.6, 109.2, 95.6, 82.5 (d, ¹J_{C12–F} = 166.8 Hz), 67.1 (d, ²J_{C12–F} = 19.1 Hz), 54.7, 26.9. ¹⁹F NMR (*d*₆-DMSO, 376 MHz) δ: –221.1 to –222.3 (m). ESI-QTOF MS *m/z*: [M + H]⁺ calcd for C₁₃H₁₅FN₂O₃, 267.1139; found, 267.1141.

2-Amino-3-(4-hydroxy-1*H*-indol-3-yl)propanoic acid (8**), 4-FEHTP Precursor (Indirect Labeling).** To an ice-cold suspension of **7** (58 mg, 0.18 mmol) and ethane-1,2-dithiol (0.18 mL, 2.17 mmol) in dichloromethane (1.8 mL) was added TFA (0.28 mL, 3.62 mmol) dropwise within 3 min, and the resulting clear, slight green solution was stirred for 10 min at 0 °C and then for 4 h at room temperature. The volatiles were then removed under reduced pressure and the residue was dried under high vacuum pump overnight. The crude was then dissolved in a mixture of MeOH (1.2 mL) and water (0.8 mL) and was purified by preparative HPLC (method E, *t*_R ≈ 9.4 min). Lyophilization of the fractions of interest yielded the title compound as a white solid (22 mg, 55%). ¹H NMR (*d*₆-DMSO, 400 MHz) δ: 10.73 (br, 1 H, H-1), 6.97 (d, ³J_{H2–H1} = 2.4 Hz, 1 H, H-2), 6.84–6.77 (m, 2 H, H-6 and H-7), 6.30 (dd, J₁ = 6.9 Hz, J₂ = 1.5 Hz, 1 H, H-5), 3.56 (dd, ³J_{H9–H8a} = 6.9 Hz, ³J_{H9–H8b} = 4.3 Hz, 1 H, H-9), 3.27 (dd, ²J_{H8a–H8b} = 15.2 Hz, ³J_{H8a–H9} = 6.9 Hz, 1 H, H-8a), 3.20 (dd, ²J_{H8b–H8a} = 15.2 Hz, ³J_{H8b–H9} = 4.3 Hz, 1 H, H-8b). ¹³C NMR (*d*₆-DMSO, 100 MHz) δ: 170.4, 151.6, 138.5, 123.0, 121.8, 117.6, 108.5, 104.8, 103.1,

55.1, 27.4. ESI-QTOF MS *m/z*: [M + Na]⁺ calcd for C₁₁H₁₂N₂O₃, 243.0740; found, 243.0741.

Methyl 2-((tert-butoxycarbonyl)amino)-3-(4-(2-((methylsulfonyl)oxy)ethoxy)-1*H*-indol-3-yl)propanoate (11**), 4-FEHTP Precursor (Direct Labeling).** General Method D. Starting from 252 mg (0.67 mmol) of **10**, *t*_R = 10.4 min (analytical HPLC, Method A), *t*_R ≈ 22 min (preparative HPLC, method D), yield 70% (213 mg). ¹H NMR (*d*₆-DMSO, 400 MHz) δ: 10.83 (br, 1 H, H-1), 7.10 (d, *J* = 7.8 Hz, 1 H, NH_{Boc}), 7.02 (br, 1 H, H-2), 6.98–6.94 (m, 2 H, H-6 and H-7), 6.51–6.45 (m, 1 H, H-5), 4.68–4.57 (m, 1 H, H-12), 4.37–4.32 (m, 2 H, H-11), 4.32–4.24 (m, 1 H, H-9), 3.61 (s, 3 H, —(C=O)OCH₃), 3.31 (dd, ²J_{H8a–H8b} = 14.0 Hz, ³J_{H8a–H9} = 4.8 Hz, 1 H, H-8a), 3.23 (s, 3 H, -OSO₂CH₃), 2.96 (dd, ²J_{H8b–H8a} = 14.0 Hz, ³J_{H8b–H9} = 10.1 Hz, 1 H, H-8b), 1.31 (s, 9 H, C(CH₃)₃ – NH_{Boc}). ¹³C NMR (*d*₆-DMSO, 100 MHz) δ: 173.3, 155.4, 152.5, 138.0, 123.1, 121.7, 116.6, 109.8, 105.4, 99.7, 78.1, 68.5, 65.7, 55.4, 51.5, 36.7, 28.3, 28.1. ESI-QTOF MS *m/z*: [M + H]⁺ calcd for C₂₀H₂₉N₂O₈S, 457.1639; found, 457.1641.

2-Amino-3-(6-(2-fluoroethoxy)-1*H*-indol-3-yl)propanoic acid (18**), 6-FEHTP.** TFA (0.17 mL, 2.18 mmol) was added dropwise to an ice-cold solution of **17** (40 mg, 0.11 mmol) in dichloromethane (1.3 mL). The resulting green reaction solution was stirred for 10 min at 0 °C and then was allowed to reach room temperature where it was stirred for 5 h. The volatiles were then removed under vacuum at 30 °C and the crude was purified with preparative HPLC with system E (*t*_R ≈ 13 min). Lyophilization of the combined relevant fractions gave the title compound as a white solid (20 mg, 69%). ¹H NMR (*d*₆-DMSO, 400 MHz) δ: 10.78 (br, 1 H, H-1), 7.44 (d, ³J_{H4–H5} = 8.7 Hz, 1 H, H-4), 7.08 (d, ³J_{H2–H1} = 2.1 Hz, 1 H, H-2), 6.88 (d, ⁴J_{H7–H5} = 2.2 Hz, 1 H, H-7), 6.67 (dd, ³J_{H5–H4} = 8.7 Hz, ⁴J_{H5–H7} = 2.2 Hz, 1 H, H-5), 4.74 (dm, 2 H, H-12), 4.20 (dm, 2 H, H-11), 3.42 (dd, ³J_{H9–H8b} = 8.7 Hz, ³J_{H9–H8a} = 4.1 Hz, 1 H, H-9), 3.25 (dd, ²J_{H8a–H8b} = 15.2 Hz, ³J_{H8a–H9} = 4.1 Hz, 1 H, H-8a), 2.93 (dd, ²J_{H8b–H8a} = 15.2 Hz, ³J_{H8b–H9} = 8.7 Hz, 1 H, H-8b). ¹³C NMR (*d*₆-DMSO, 100 MHz) δ: 169.9, 154.3, 136.9, 122.9, 122.1, 119.1, 109.7, 108.8, 95.7, 82.4 (d, ¹J_{C12–F} = 166.5 Hz), 67.5 (d, ²J_{C11–F} = 19.1 Hz), 54.7, 27.2. ¹⁹F NMR (*d*₆-DMSO, 376 MHz) δ: –224.8 to –223.7 (m). ESI-QTOF MS *m/z*: [M + H]⁺ calcd for C₁₃H₁₅FN₂O₃, 267.1139; found, 267.1143.

2-Amino-3-(6-hydroxy-1*H*-indol-3-yl)propanoic acid (19**), 6-FEHTP Precursor (Indirect Labeling).** A solution of lithium hydroxide hydrate (170 mg, 4.1 mmol) in water (9.2 mL) was added dropwise within 10 min to a solution of **14** (464 mg, 1.98 mmol) in THF (18.4 mL) and i-PrOH (4.6 mL) at 5 °C. The reaction mixture was stirred for 6 h at this temperature (slightly varying within this time 5–7 °C). The reaction was then neutralized by adding HCl 0.2 N (approximately 10 mL, pH ≈ 6), and the volatiles were removed under reduced pressure to a final volume of ≈4 mL. The grayish precipitate was filtered off, washed thoroughly with cold water, and dried under vacuum to yield the title compound (256 mg, 59%). ¹H NMR (*d*₆-DMSO, 400 MHz) δ: 10.46 (br, 1 H, H-1), 7.30 (d, ³J_{H4–H5} = 8.5 Hz, 1 H, H-4), 6.96 (d, ³J_{H2–H1} = 2.1 Hz, 1 H, H-2), 6.69 (d, ⁴J_{H7–H5} = 2.1 Hz, 1 H, H-7), 6.51 (dd, ³J_{H5–H4} = 8.5 Hz, ⁴J_{H5–H7} = 2.1 Hz, 1 H, H-5), 3.36 (dd, ³J_{H9–H8b} = 9.1 Hz, ³J_{H9–H8a} = 3.8 Hz, 1 H, H-9), 3.23 (dd, ²J_{H8a–H8b} = 15.4 Hz, ³J_{H8a–H9} = 3.8 Hz, 1 H, H-8a), 2.85 (dd, ²J_{H8b–H8a} = 15.4 Hz, ³J_{H8b–H9} = 9.1 Hz, 1 H, H-8b). ¹³C NMR (*d*₆-DMSO, 100 MHz) δ: 169.8, 153.1, 137.5, 121.7, 120.7, 118.7, 109.6, 96.4,

54.7, 27.3. ESI-QTOF MS m/z : [M + Na]⁺ calcd for C₁₁H₁₂N₂O₃, 243.0746; found, 243.0742.

Methyl 2-((tert-butoxycarbonyl)amino)-3-(6-(2-((methylsulfonyl)oxy)ethoxy)-1H-indol-3-yl)propanoate (22), 6-FEHTP Precursor, (Direct Labeling). General method D. Starting from 137 mg of **21**, $t_R = 10.7$ min (analytical HPLC, method A), $t_R \approx 25$ min (preparative HPLC, method D), yield 97 mg (59%). ¹H NMR (d_6 -DMSO, 400 MHz) δ : 10.68 (br, 1 H, H-1), 7.37 (d, $^3J_{H4-H5} = 8.6$ Hz, 1 H, H-4), 7.17 (d, $J = 7.8$ Hz, 1 H, NH_{Boc}), 7.03 (br, 1 H, H-2), 6.88 (d, $^4J_{H7-H8} = 2.1$ Hz, 1 H, H-7), 6.70 (dd, $^3J_{H5-H4} = 8.6$ Hz, $^4J_{H5-H7} = 2.1$ Hz, 1 H, H-5), 4.57–4.51 (m, 2 H, H-12), 4.27–4.14 (m, 3 H, H-11 and H-9), 3.59 (s, 3 H, C(=O)OCH₃), 3.24 (s, 3 H, -OSO₂CH₃), 3.06 (dd, $^2J_{H8a-H8b} = 14.6$ Hz, $^3J_{H8a-H9} = 5.4$ Hz, 1 H, H-8a), 2.96 (dd, $^2J_{H8b-H8a} = 14.6$ Hz, $^3J_{H8b-H9} = 9.0$ Hz, 1 H, H-8b), 1.34 (s, 9 H, C(CH₃)₃ – NH_{Boc}). ¹³C NMR (d_6 -DMSO, 100 MHz) δ : 172.9, 155.3, 154.0, 136.6, 122.6, 121.9, 118.7, 109.8, 108.9, 95.8, 78.2, 69.0, 66.1, 54.7, 51.7, 36.8, 28.1, 26.9. ESI-QTOF MS m/z : [M + Na]⁺ calcd for C₂₀H₂₈N₂O₈S, 479.1459; found, 479.1461

2-Amino-3-(7-(2-fluoroethoxy)-1H-indol-3-yl)propanoic acid (28), 7-FEHTP. TFA (0.24 mL, 3.2 mmol) was added dropwise to an ice cold solution of **27** (58 mg, 0.16 mmol) in dichloromethane (2 mL). The resulting green reaction solution was stirred for 10 min at 0 °C and then was allowed to reach room temperature where it was stirred for 5 h. Toluene was then added, and the volatiles were removed under reduced pressure. The residue was dried over high vacuum to provide the title compound as a yellowish oil, sufficiently pure by NMR. ¹H NMR (CD₃OD, 400 MHz) δ : 7.24 (bd, $^3J_{H4-H5} = 7.8$ Hz, 1 H, H-4), 7.18 (s, 1 H, H-2), 6.99 (t, $^3J_{H5-H4} = ^3J_{H5-H6} = 7.8$ Hz, 1 H, H-5), 6.69 (d, $^3J_{H6-H5} = 7.8$ Hz, 1 H, H-6), 4.81 (dm, $^2J_{H12-F} = 47.7$ Hz, 2 H, H-12), 4.37 (dm, $^3J_{H11-F} = 29$ Hz, 2 H, H-11), 4.24 (dd, $^3J_{H9-H8a} = 7.9$ Hz, $^3J_{H9-H8b} = 4.8$ Hz, 1 H, H-9), 3.48 (dd, $^2J_{H8b-H8a} = 15.3$ Hz, $^3J_{H8b-H9} = 4.8$ Hz, 1 H, H-8B), 3.31 (dd, $^2J_{H8a-H8b} = 15.3$ Hz, $^3J_{H8a-H9} = 7.9$ Hz, 1 H, H-8A). ¹³C NMR (CD₃Cl, 100 MHz) δ : 168.2, 144.8, 133.7, 124.0, 120.7, 112.9, 110.5, 109.6, 104.2, 83.6 (d, $^1J_{C12-F} = 168.8$ Hz), 69.2 (d, $^2J_{C11-F} = 20$ Hz), 56.3, 28.9. ESI-QTOF MS m/z : [M + H]⁺ calcd for C₁₈H₂₃FN₂O₅, 267.1139; found, 267.1140.

Radiosynthesis. For the radiosynthesis of [¹⁸F]4-FEHTP and [¹⁸F]6-FEHTP, both indirect and direct approaches were used, whereas in the case of [¹⁸F]7-FEHTP, only the indirect approach was followed. The indirect approach was similar to the one already established in our lab.²⁰ The disodium salts of the corresponding hydroxytryptophans were prepared by reacting these with 2 equiv of sodium methoxide (0.5 N) in dry methanol at room temperature. After evaporation of the solvent, the resulting salts were stored at –25 °C and were stable over time, as shown by NMR analysis.

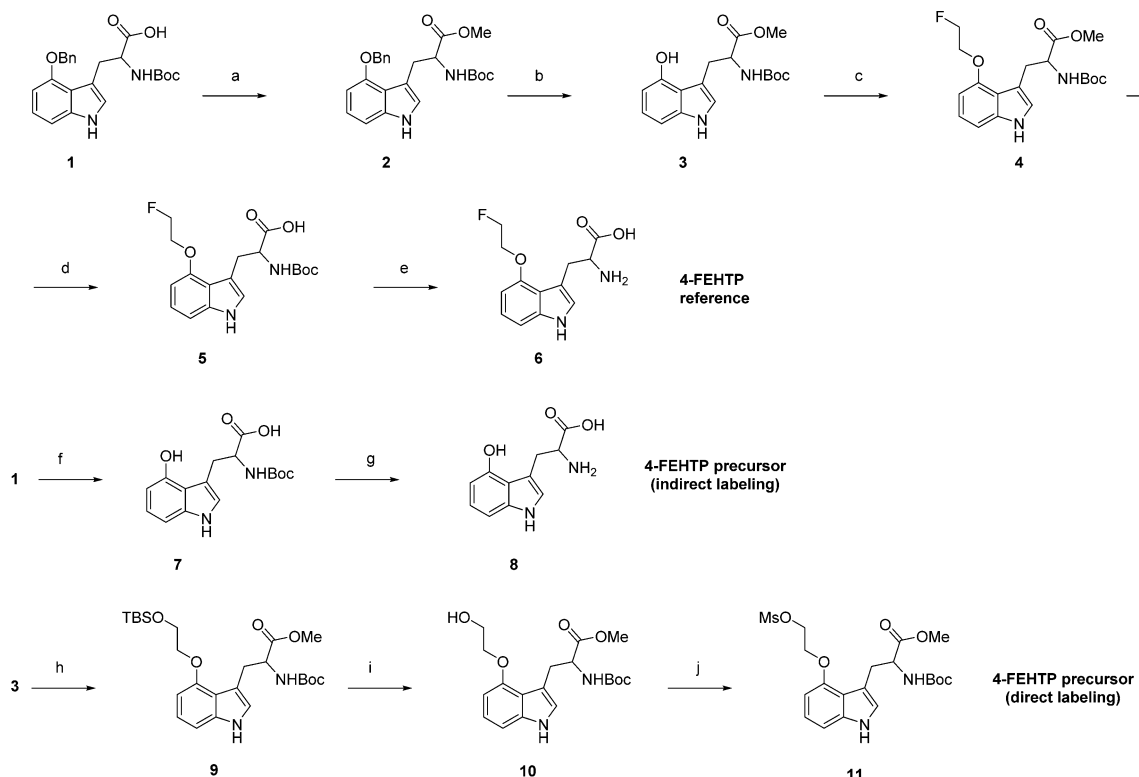
For the indirect labeling approach, no-carrier-added ¹⁸F-fluoride was produced via the ¹⁸O(p,n)¹⁸F nuclear reaction by irradiation of enriched ¹⁸O-water in a cyclotron (Cyclone 18/9, IBA). ¹⁸F[–] was trapped on a light QMA cartridge (Waters), which was preconditioned with 0.5 M K₂CO₃ (5 mL) and water (5 mL). The activity was eluted with tetrabutylammonium hydroxide (0.6 mL, 0.18 mM in methanol), and the solvent was evaporated at 110 °C under vacuum in the presence of slight inflow of nitrogen gas. After addition of acetonitrile (0.6 mL), azeotropic drying was carried out. This procedure was repeated twice to afford dry [¹⁸F]TBAF. To the dried ¹⁸F, ethylene glycol ditosylate (5–6 mg in 0.7 mL MeCN) was added, and

the mixture was heated at 85 °C for 6 min. The reaction mixture was cooled, diluted with 35% ethanol in water (10 mL) and passed through a LiChrolute EN cartridge (Merck). The cartridge was washed with 0.3 mL of DMSO, which was discarded, and the labeled product [¹⁸F]-2-fluoroethyltosylate was eluted with 0.8 mL DMSO to the second reactor, which had been preloaded with the disodium salt of the corresponding hydroxytryptophan (~5 mg) in a mixture of water (0.1 mL) and DMSO (0.2 mL). The reaction mixture was heated at 120 °C for 8 min, and after cooling, it was diluted with water (2 mL) and purified by semipreparative HPLC. [¹⁸F]7-FEHTP was collected at about 16 min, and [¹⁸F]6-FEHTP eluted at about 13 min and neutralized with sodium hydrogen carbonate 10%. In the [¹⁸F]6-FEHTP solution, sodium ascorbate was added to a final concentration of 10–20 mg/mL. The solutions were passed through a sterile filter and used for the in vitro and in vivo studies. This method failed to give the correct [¹⁸F]4-FEHTP tracer.

For the direct labeling approach, ¹⁸F[–] was initially trapped on a light QMA cartridge (Waters), which was preconditioned with 0.5 M K₂CO₃ (5 mL) and water (5 mL). A 1 mL volume of Kryptofix K_{2.2.2}/K₂CO₃ solution (Kryptofix K_{2.2.2}; 5 mg, K₂CO₃, 1 mg in MeCN (1.4 mL)/water (0.6 mL)) was used for the elution of ¹⁸F[–] from the cartridge. The solvents were evaporated at 110 °C under vacuum in the presence of slight inflow of nitrogen gas, and azeotropic drying was carried out twice with the addition of 0.5 mL acetonitrile each time, to afford dry [¹⁸F]KF-K_{2.2.2}. A solution of the corresponding mesylate precursor (~5 mg in 0.6 mL dry acetonitrile) was added to the dried [¹⁸F]KF-K_{2.2.2} complex, and the reaction mixture was heated at 100 °C for 10 min and then evaporated to dryness under reduced pressure with a slight inflow of nitrogen. To the crude material was added HCl 4 M solution (0.6 mL), and the reaction was heated at 100 °C for 10 min. The mixture was then neutralized by the addition of NaOH 4 M solution (0.57 mL) and PBS 0.6 M (1.4 mL) containing 20 mg/mL sodium ascorbate (final pH ≈ 6). Purification was performed by semipreparative HPLC, with [¹⁸F]4-FEHTP eluting at about 18 min and [¹⁸F]6-FEHTP at 13 min. Each product was collected in a vial containing 40 mg of sodium ascorbate. The products were neutralized with sodium hydrogen carbonate (10%) to pH ≈ 6 and diluted with saline to afford the final formulation, containing 20 mg/mL sodium ascorbate. The solutions were then passed through a sterile filter and used for in vitro and in vivo studies.

Identification of [¹⁸F]4-FEHTP, [¹⁸F]6-FEHTP, and [¹⁸F]7-FEHTP was confirmed by coinjection with reference compounds **6**, **18**, and **28** respectively. Chemical and radiochemical purity were determined by analytical HPLC; $t_R = 10.7$ min for [¹⁸F]4-FEHTP, 10.3 min for [¹⁸F]6-FEHTP and 10.5 for [¹⁸F]7-FEHTP. The radiochemical purity of the biologically tested tracers was always ≥95%. [¹⁸F]L-FET was obtained from a routine clinical production from the University Hospital Zurich, Switzerland.

In Vivo PET Studies. Animal care and experiments were conducted in accordance with Swiss Animal Welfare legislation and were approved by the Veterinary Office of the Canton Zurich, Zurich, Switzerland. Five weeks old female NMRI nude mice (Charles River, Sulzfeld, Germany) were inoculated subcutaneously in the right shoulder region with 10⁷ NCI-H69 cells (Cell Lines Service, Eppelheim, Germany) in 100 μL of Matrigel (BD Biosciences). Xenografts were grown for 2 weeks until they reached a volume between 0.5 to 1 cm³.

Scheme 1. Synthesis of 4-FEHTP and Corresponding Precursors^a

^aReagents and conditions: (a) TMSCH₂N₂, benzene/methanol 1:1, room temperature, 3.5 h, 57%; (b) 20% Pd(OH)₂/C – cyclohexene, ethanol, reflux, 2 h, 80%; (c) FCH₂CH₂OTs, Cs₂CO₃, DMF, 60 °C, 2.5 h, 84%; (d) LiOH, THF/H₂O/i-PrOH 4:2:1, 0–15°C, 3.5 h, 93%; (e) TFA, dichloromethane, 0°C then room temperature, 16 h, 49%; (f) 20% Pd(OH)₂/C – cyclohexene, ethanol, reflux, 18 h, 75%; (g) TFA, ethane-1,2-dithiol, dichloromethane, 0°C then room temperature, 4 h, 55%; (h) TsOCH₂CH₂OTBS, Cs₂CO₃, DMF, 55–60 °C, 3 h, 77%; (i) TBAF 1M in THF, THF, room temperature, 90 min, 90%; (j) mesyl chloride, Et₃N, DCM, 0°C, 40 min, 70%.

Anesthesia with 2%–3% isoflurane in oxygen-air was initiated 10 min before PET acquisition, and mice were monitored as previously described.²¹ PET scans were performed with the dedicated small animal PET/CT camera Vista eXplore (Sedecal, Spain) in list mode for dynamic analysis starting at 1 or 60 min p.i. of 10–14 MBq radiotracer and lasted for 90 min. Data were reconstructed with the 2D ordered-subsets expectation maximization (2D-OSEM) protocol and analyzed with PMOD v3.5 software (PMOD Technologies Ltd.). Volumes of interest for the xenograft and reference region on the contralateral side (muscle) were drawn in PMOD on the basis of the PET images. Standardized uptake values (SUV) were calculated as the ratio of regional averaged radioactivity in Becquerel per cubic centimeter and injected radioactivity in Becquerel per gram body weight.

Ex Vivo Metabolite Studies. [¹⁸F]6-FEHTP (89–95 MBq) was injected via a lateral tail vein into 10 weeks old female NMRI nu/nu mice bearing NCI-H69 xenografts. Blood samples were withdrawn via the opposite tail vein, and animals were sacrificed by decapitation under isoflurane anesthesia at the indicated time points. Blood was collected in heparinized tubes and centrifuged to separate blood cells and plasma. Xenografts were excised, homogenized in PBS, and centrifuged. The resulting supernatants and blood plasma were mixed with an equal volume ice cold acetonitrile to precipitate the proteins, followed by centrifugation at 5000g, 4 °C for 5 min. Supernatants were filtered through 0.2 μm filters and analyzed by radio TLC. Normal phase TLC plates were used (aluminum sheets, silica gel 60 F₂₅₄, Merck). The mobile phase was DCM/

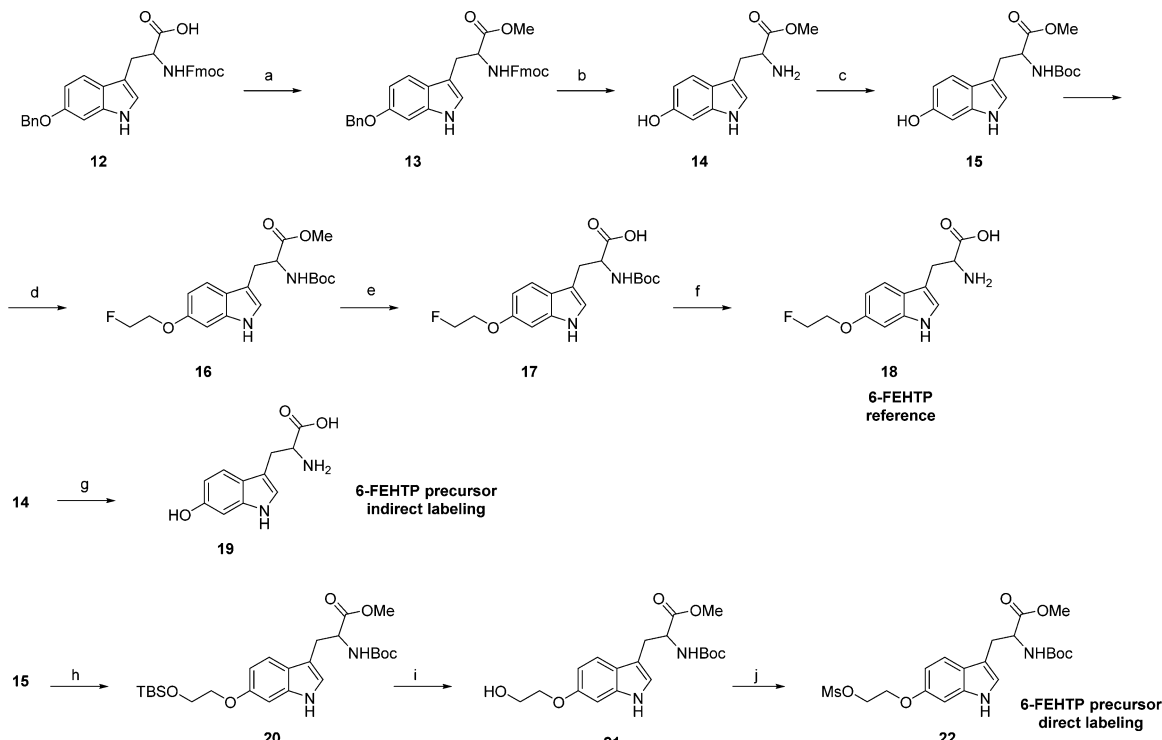
MeOH/NH₄OH (25%) 70:30:3. Developed TLCs were visualized with InstantImager (Canberra Packard). Conditions for UPLC analysis were the same as for radiosynthesis control.

In Vitro Cell Uptake and Inhibition Studies. In vitro cell uptake and efflux experiments were performed with NCI-H69 cells as previously described with some modifications.^{20,21} In brief, cells were cultivated in 300 cm² flasks and split 1:1 24 h before the experiment. Before the experiment, cells were washed twice and incubated in 5 mL plastic tubes at 37 °C, 120 rpm with the indicated buffer/electrolyte for 1 h. At time zero, 0.1 mM monoamine oxidase inhibitors clorgyline, pargyline and 20 kBq [¹⁸F]6-FEHTP were added. To investigate the influence of Na⁺ and BCH on cell uptake, Na⁺-free buffer (1.8 mM CaCl₂, 0.8 mM MgSO₄, 5.3 mM KCl, 5.5 mM D-glucose, pH 7.4) was supplemented with either 117 mM choline chloride or 117 mM NaCl (Na⁺-containing buffer) as well as 10 mM BCH as indicated. Additional experiments with and without 80 μM AADC inhibitor S-carbidopa (Santa Cruz Biotechnology) were performed with Earle balanced salt solution containing Ca²⁺ and Mg²⁺ (EBSS, Invitrogen).

Statistical Analysis. Cell uptake and PET SUV ratios between xenografts and reference tissue were analyzed by two-tailed homoscedastic Student's *t* test. A statistic value of *P* < 0.05 was considered as significant. Average values are shown with standard deviations or data range in the case of *n* = 2.

RESULTS AND DISCUSSION

Chemistry. The synthesis of the cold analogues 4-FEHTP, 6-FEHTP, and 7-FEHTP and corresponding precursors are

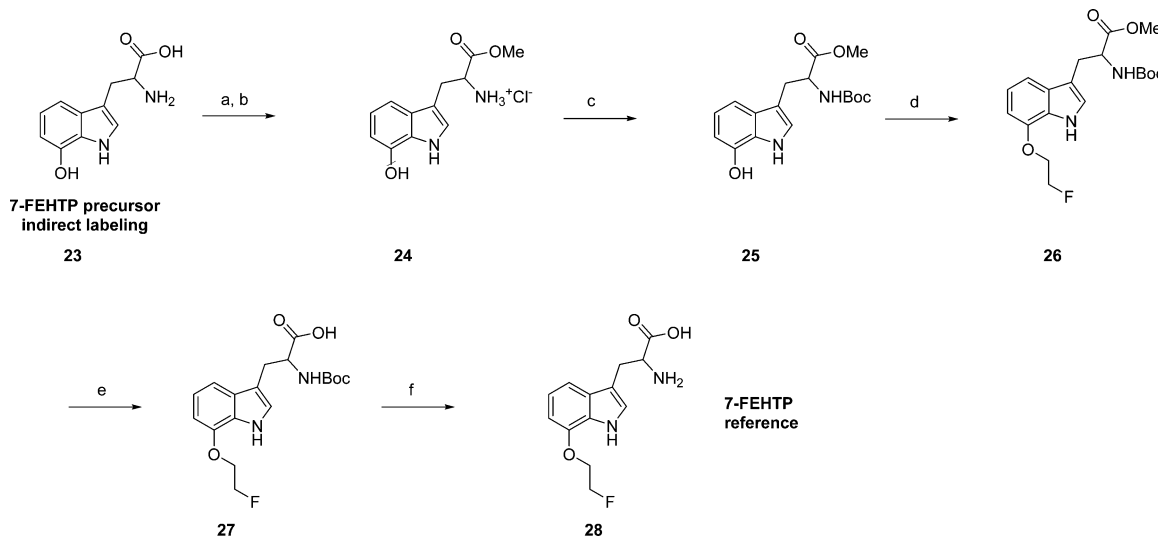
Scheme 2. Synthesis of 6-FEHTP and Corresponding Precursors^a

^aReagents and conditions: (a) TMSCH₂N₂, benzene/methanol 1:1, room temperature, 3.5 h, 75%; (b) 20% Pd(OH)₂/C – cyclohexene, ethanol, reflux, 8 h, 95%; (c) Boc anhydride, triethylamine, dichloromethane/methanol, 0°C to room temperature, 2.5 h, 88%; (d) FCH₂CH₂OTs, Cs₂CO₃, DMF, 55–60°C, 5 h, 57%; (e) LiOH, THF/H₂O/i-PrOH 4:2:1, 5°C, 3 h, 91%; (f) TFA, dichloromethane, 0°C then room temperature, 5 h, 69%; (g) LiOH, THF/H₂O/i-PrOH 4:2:1, 5°C, 6 h, 59%; (h) TsOCH₂CH₂OTBS, Cs₂CO₃, DMF, 55–60 °C, 6 h, 65%; (i) TBAF 1M in THF, THF, room temperature 90 min, 98%; (j) mesyl chloride, Et₃N, DCM, 0°C, 60 min, 59%.

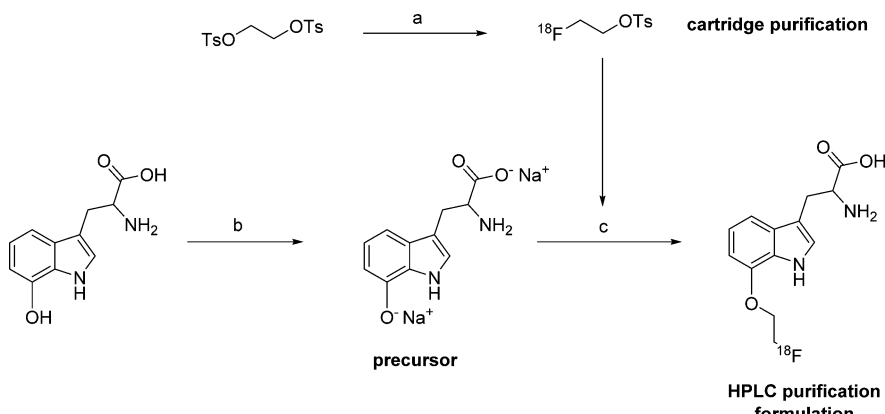
shown in Schemes 1–3, respectively. We used racemic DL-tryptophan analogues as we initially wanted to verify whether the new analogues would show any remarkable biological performance. For 4-FEHTP, the protected analogue of 4-hydroxytryptophan **1** was treated with TMS diazomethane in a mixture of methanol and benzene to give the corresponding methyl ester **2** in 57% yield. The benzyl group was then cleaved by transfer hydrogenation with 20% Pd(OH)₂/C and cyclohexene in ethanol³⁴ to yield the free phenol **3** (80%) which was then O-alkylated with 2-fluoroethyl tosylate and cesium carbonate in DMF to provide the corresponding fluoroethoxy tryptophan compound **4** in good yield (84%). Subsequently, the methyl ester was cleaved with LiOH in THF/water/i-PrOH to afford the free acid **5** in 93% yield, and the remaining Boc group was removed with TFA in DCM to give the final reference compound 4-FEHTP (**6**) in 43% after HPLC purification. For radiosynthesis, precursor **8** (4-hydroxytryptophan) was first synthesized to be used for indirect labeling (alkylation reaction of 4-hydroxytryptophan with [¹⁸F]2-fluoroethyltosylate). For this, debenzylation of the starting material **1** with transfer hydrogenation and subsequent treatment with TFA afforded **8** in a modest overall yield. Unfortunately, this precursor failed to give the desired [¹⁸F]4-FEHTP (see the section named Radiosynthesis) and thus, a new precursor was synthesized to be used for direct labeling. Toward this direction, phenol **3** was alkylated with 2-(*tert*-butyldimethylsilyl)oxyethyl 4-methylbenzenesulfonate in DMF with cesium carbonate to give the TBS protected analogue **9** in 77% yield. Interestingly, attempts to obtain directly the free alcohol **10** by reacting phenol **3** with 2-

bromoethanol or 2-tosylethanol failed to give the correct product, probably because of the presence of the unprotected alcohol. Additionally, Mitsunobu reaction with 2-tosyl ethanol also failed to give directly the desired sulfonate precursor. On the other hand, cleavage of the TBS group of **9** with TBAF in THF smoothly afforded alcohol **10** in excellent yield (90%). The alcohol was subsequently reacted with mesyl chloride with triethylamine in DCM to provide sulfonate **11**, which was purified by preparative HPLC to afford the final precursor in satisfactory yield (70%).

6-FEHTP was synthesized by following a similar synthetic procedure described for 4-FEHTP starting from the Fmoc/Bn protected analogue **12**. Again the methyl ester was introduced with TMS diazomethane to afford **13** in 75% yield. During the subsequent transfer hydrogenolysis step, monitoring of the reaction by TLC showed that at the time the starting material was completely consumed, a very polar byproduct was also present, which was identified with LRMS as the corresponding compound, where cleavage of the Fmoc protection group had also occurred. Despite the common belief that the Fmoc group is fairly stable toward hydrogenolysis, there are some examples in the literature where instability under hydrogenation conditions is observed.³⁵ Debenzylation was faster than Fmoc cleavage, but unfortunately, after workup, substantial cleavage of the Fmoc group was observed, presumably through autocatalysis by the liberated amine upon concentration of the reaction mixture. Other hydrogenating systems (10% Pd/C and cyclohexadiene in ethanol)³⁶ failed to increase selectivity, and thus, it was decided to prolong the reaction time so as to achieve full Fmoc deprotection with parallel debenzylation and

Scheme 3. Synthesis of 7-FEHTP^a

^aReagents and conditions: (a) HCl (1.25 M in MeOH), 0 °C, 15 min, (b) SOCl₂, MeOH, 0°C then reflux, 3 h, quantitative; (c) Boc anhydride, triethylamine, DCM, 0°C to room temperature, 8 h, 72%; (d) 2-fluoroethanol, DEAD/PPh₃, DCM, room temperature, 16 h, 81%; (e) LiOH, THF/H₂O/i-PrOH 4:2:1, 5°C, 3 h, 94%; (f) TFA, dichloromethane, 0°C then room temperature, 16 h, quantitative.

Scheme 4. Example of the Indirect Labeling Approach for [¹⁸F]7-FEHTP^a

^aReagents and conditions: (a) [¹⁸F]TBAF, MeCN, 85 °C, 6 min; (b) MeONa, MeOH, room temperature, 10 min; (c) DMSO/H₂O, 120 °C, 8 min. Same methodology was used for the rest of the analogues. This method failed to give the correct product for [¹⁸F]4-FEHTP.

incorporate a Boc group at the following step. Indeed, refluxing the reaction mixture for 6 h led to full cleavage of the Fmoc group, and the free amine/phenol **14** was isolated in 95% yield after purification. Compound **14** was then treated with Boc anhydride/triethylamine in DCM which afforded the corresponding Boc-protected analogue **15**, which was subsequently reacted with 2-fluoroethyltosylate in DMF to give the alkylated analogue **16** in 57% yield. Finally, cleavage of the methyl ester and the Boc group as in the case of the 4-FEHTP afforded the final reference compound 6-FEHTP (**18**) in moderate yield. For the radiosynthesis of [¹⁸F]6-FEHTP, two different precursors were synthesized. 6-Hydroxytryptophan (**19**) would be used for indirect labeling and was synthesized by treating **14** with LiOH, which afforded the desired precursor in satisfactory yield (59%). For the direct approach, the protected mesyl precursor **22** was synthesized, starting from compound **15** and following the same methodology as described for 4-FEHTP (Scheme 2).

7-FEHTP was synthesized from 7-hydroxytryptophan (**23**). The starting material was first converted to its hydrochloric salt

and then reacted with thionyl chloride in methanol to obtain the corresponding methyl ester **24** in quantitative yield. Methyl ester **24** was subsequently protected with a Boc group by reacting it with Boc anhydride/triethylamine in DCM to afford compound **25** in 72% yield. The protected phenol was then coupled with 2-fluoroethanol via Mitsunobu reaction with DEAD/PPh₃ in DCM which afforded 7-fluoroethoxy tryptophan **26** in good yield (81%). Finally, as in the previous cases, cleavage of the methyl ester with lithium hydroxide followed by TFA Boc deprotection yielded the reference compound 7-FEHTP **28**. 7-Hydroxytryptophan was used as the precursor for indirect labeling which yielded [¹⁸F]7-FEHTP in a reliable way (Scheme 3).

Radiochemistry. For the radiosyntheses of all new fluoroethoxy analogues, we initially decided to follow an indirect labeling approach, shown in Scheme 4, as this was already previously established in our lab for [¹⁸F]L-FEHTP.²⁰ This method involves first nucleophilic [¹⁸F] fluorination of ethylene glycol ditosylate to yield [¹⁸F]2-fluoroethyltosylate. After a quick purification procedure, the labeled intermediate

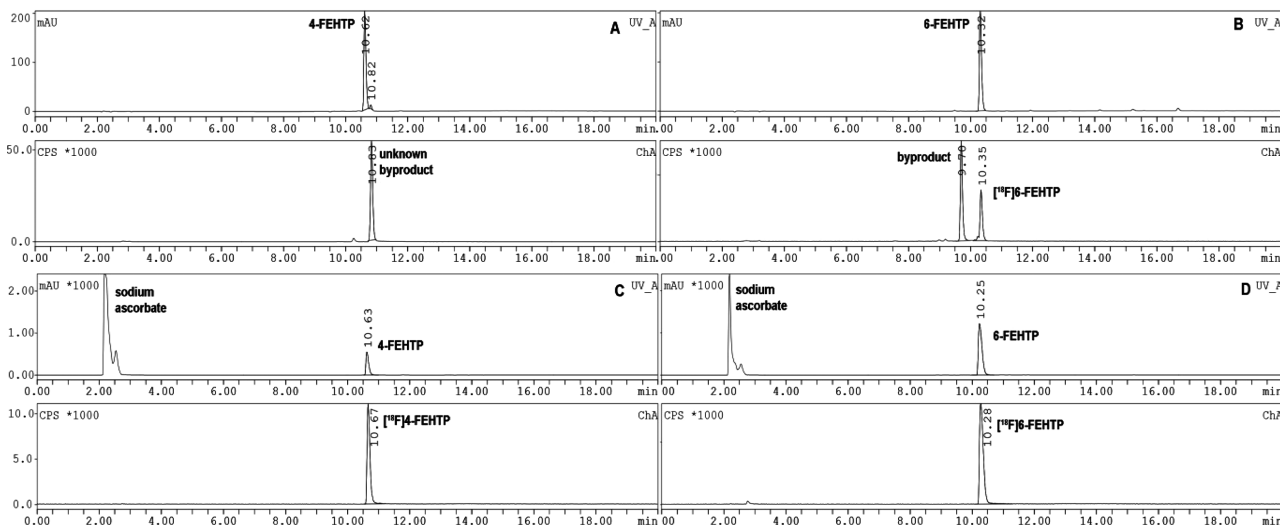
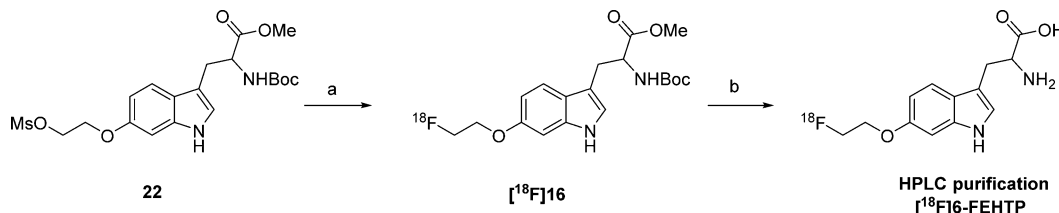


Figure 3. Quality control (coinjections) for $[^{18}\text{F}]$ 4-FEHTP and $[^{18}\text{F}]$ 6-FEHTP with two different radiolabeling methods. (A) Indirect method for $[^{18}\text{F}]$ 4-FEHTP where the isolated product does not correspond with the reference ($\Delta t_R > 0.2$ min when usually $0.08 \text{ min} \geq \Delta t_R \geq 0.02$ min). (B) Indirect method for $[^{18}\text{F}]$ 6-FEHTP where the major labeled product does not correspond to the reference compound, although a single peak was isolated with semiprep purification. (C) Direct method for $[^{18}\text{F}]$ 4-FEHTP. (D) Direct method for $[^{18}\text{F}]$ 6-FEHTP.

Scheme 5. Example of the Direct Labeling Approach for $[^{18}\text{F}]$ 6-FEHTP^a



^aReagents and conditions: (a) $[^{18}\text{F}]$ KF-K_{2.2.2}, MeCN, 100 °C, 10 min; (b) HCl (4M), 100 °C, 10 min. The same methodology was used for $[^{18}\text{F}]$ 4-FEHTP.

was transferred to a second reaction vial where it was coupled to the disodium salt of the corresponding hydroxy-tryptophan by heating at 120 °C in DMSO/water. The reaction mixture was purified by semipreparative HPLC. Although this approach proved efficient and reliable for the case of $[^{18}\text{F}]$ -7FEHTP, it failed to give the correct tracer for $[^{18}\text{F}]$ 4-FEHTP as quality control of the final purified product revealed that its retention time did not match with the reference compound (Figure 3A). For $[^{18}\text{F}]$ 6-FEHTP, the method did not reliably provide a pure tracer as sometimes quality control of the single isolated peak obtained by semiprep purification revealed the presence of a slightly more polar peak contaminating the $[^{18}\text{F}]$ 6-FEHTP tracer in an unacceptable amount (Figure 3B).

All these discrepancies could possibly be attributed to the competing nucleophilicity of other functional groups present in the structures of the precursors. Among these, alkylation at the N-1 position of the indole core would lead to N-1 alkylated fluoroethoxy analogues, which could potentially have similar retention times with the O-alkylated ones due to their structural similarity and thus maybe not easily separable by semipreparative HPLC. Structures where alkylation has taken place at the carboxyl or amino part are most probably excluded as this kind of structural modification would have great impact on the polarity of the molecules with major differences in retention time. In addition, the different localization of the hydroxyl group on the tryptophan ring is bound to have an effect on the acidity of the corresponding hydroxy-tryptophan

(and thus its nucleophilicity), which could explain why such inconsistencies were not observed in the case of $[^{18}\text{F}]$ 7-FEHTP, although they were common for $[^{18}\text{F}]$ 4-FEHTP and $[^{18}\text{F}]$ 6-FEHTP. Finally, although NMR analysis confirmed that the disodium salts of all precursors are stable with time, the possibility exists that they might be oxidized during the labeling reaction leading to labeled byproducts not easily separable by preparative HPLC.

In order to circumvent this problem, new precursors were synthesized for $[^{18}\text{F}]$ 4-FEHTP and $[^{18}\text{F}]$ 6-FEHTP, to be used for the direct labeling approach, following a similar method used for our previously synthesized $[^{18}\text{F}]$ 2-FPTRP and $[^{18}\text{F}]$ 5-FPTRP.²¹ This method includes a two-step reaction sequence involving nucleophilic fluorination of the corresponding protected mesylate precursors (**9** and **22**) and subsequent deprotection as presented in Scheme 5. Nucleophilic substitution was achieved by heating the corresponding mesylate precursors with $[^{18}\text{F}]$ KF-K_{2.2.2} in acetonitrile at 100 °C for 10 min. After removal of the solvent, deprotection was accomplished in the same reaction vial through the addition of HCl 4 M and heating again at 100 °C for 10 min. The solution was carefully neutralized and purified by semipreparative HPLC. The peaks were collected and neutralized to pH ≈ 6 and sodium ascorbate was added to prevent radiolysis, as it was observed that these two tracers were not stable in this formulation without the addition of an antioxidant. This was not observed for $[^{18}\text{F}]$ 7-FEHTP. Unlike the indirect approach,

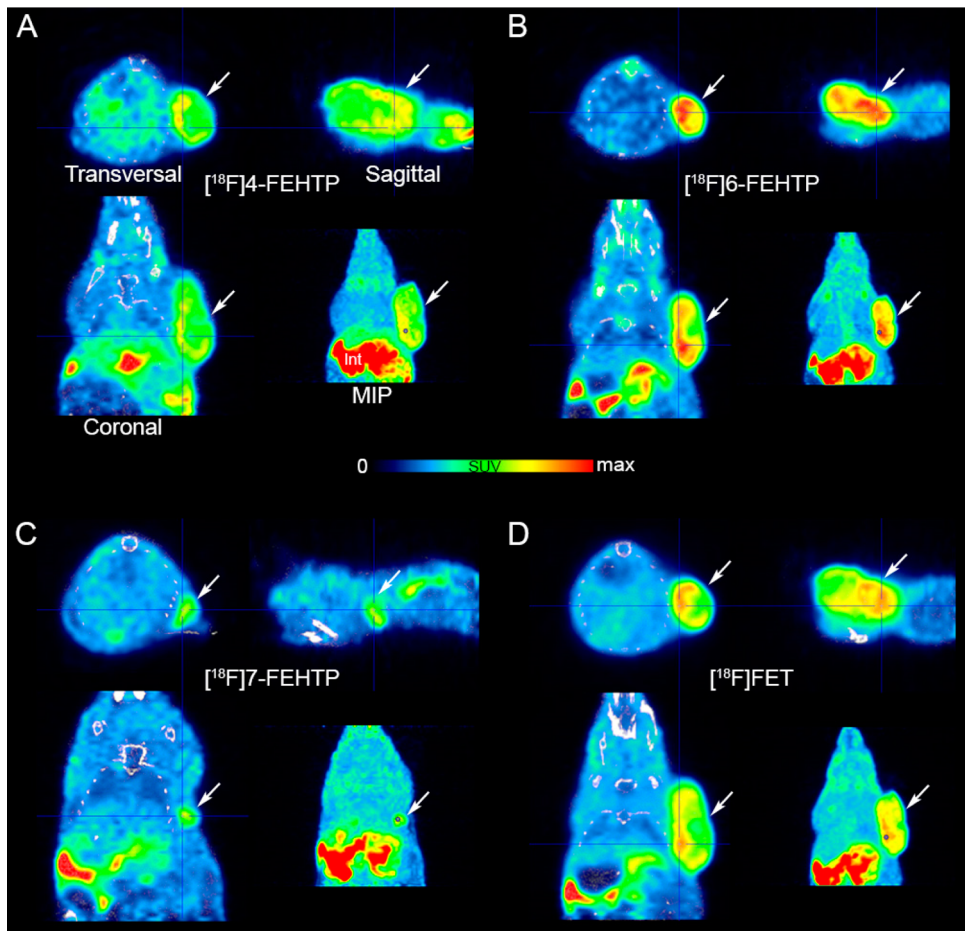


Figure 4. PET/CT images of NCI-H69 xenograft-bearing mice after intravenous injection of 10–14 MBq $[^{18}\text{F}]$ 4-FEHTP (A), $[^{18}\text{F}]$ 6-FEHTP (B), $[^{18}\text{F}]$ 7-FEHTP (C), and $[^{18}\text{F}]$ L-FET (D). PET data are averaged from 60 to 75 min post tracer injection, when xenograft-to-reference ratios were highest. Note: animal is the same in A, B, and D. SUV scales are adjusted to result in similar color (blue) for background tissue in all images. Maximal (max) SUV are 1.3 (A), 1.4 (B), 1.8 (C), and 2.7 (D). CT in white/gray. Arrows indicate xenografts. MIP, maximal intensity projection; Int, intestines. Cross hairs indicate optical planes. Anatomical left is left in images.

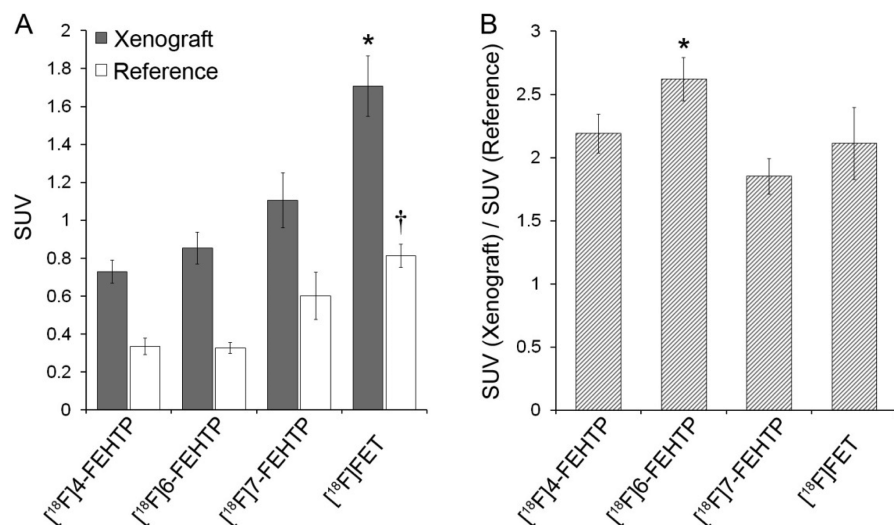


Figure 5. Standardized uptake values (SUVs) of NCI-H69 xenografts and reference regions (A) and SUV ratios of xenograft-to-reference region (B) after $[^{18}\text{F}]$ 4-FEHTP ($n = 6$), $[^{18}\text{F}]$ 6-FEHTP ($n = 8$), $[^{18}\text{F}]$ 7-FEHTP ($n = 2$, end of error bars indicate both data values), and $[^{18}\text{F}]$ L-FET ($n = 9$) injection. SUVs represent PET data averaged between 60 to 75 min post-tracer injections. SUV of $[^{18}\text{F}]$ L-FET xenograft relative to SUV-xenograft of all other radiotracers: * $P < 0.001$; SUV of $[^{18}\text{F}]$ L-FET-reference relative to SUV-reference region of all other radiotracers: † $P < 0.005$; SUV ratio of $[^{18}\text{F}]$ 6-FEHTP relative to all other radiotracers: * $P < 0.001$.

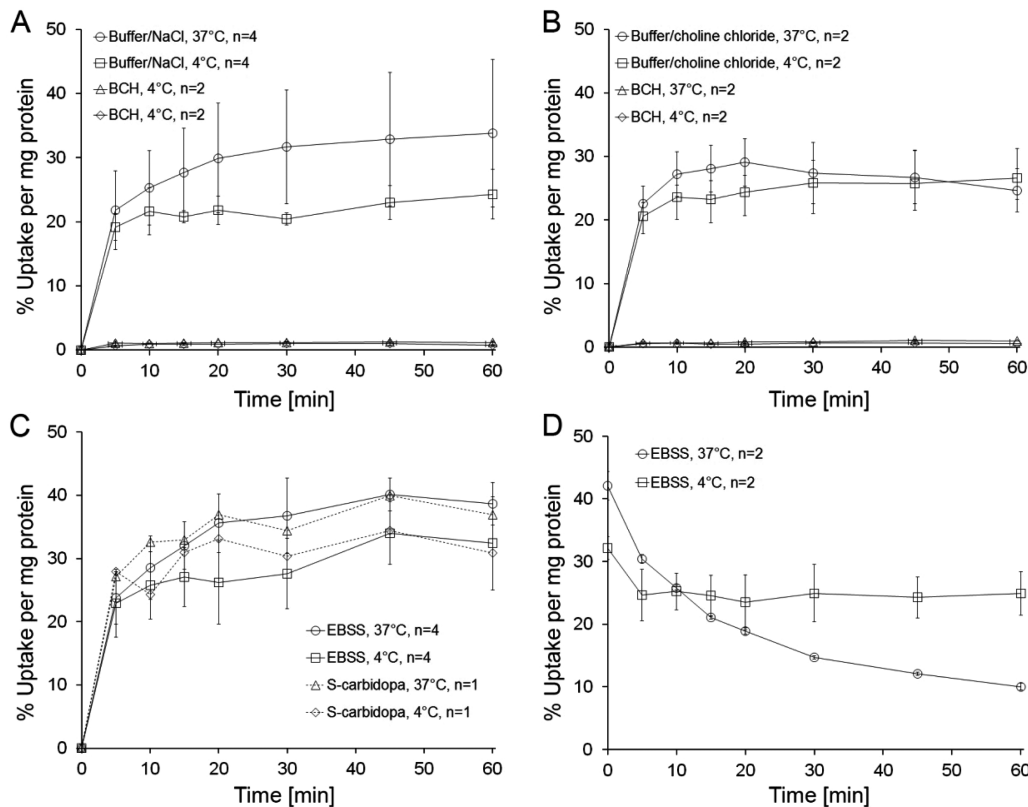


Figure 6. Uptake (A–C) and efflux (D) of $[^{18}\text{F}]6\text{-FEHTP}$ in NCI-H69 cells. (A) Uptake in Na^+ -containing HEPES/TRIS buffer at 37 and 4 °C with and without 10 mM LAT1/2 inhibitor BCH as indicated. (B) As in (A) but in the absence of Na^+ . (C) Uptake in EBSS with and without 80 μM AADC inhibitor S-carbidopa as indicated in Figure. (D) Efflux of $[^{18}\text{F}]6\text{-FEHTP}$ in EBSS in the absence of added amino acids. For all experiments with $n = 2$, error bars indicate values of individual experiments.

this method consistently yielded the desired tracers $[^{18}\text{F}]4\text{-FEHTP}$ and $[^{18}\text{F}]6\text{-FEHTP}$ (Figures 3C,D), and their identity was established by coinjection with reference compounds **6** and **18**, respectively. Chemical and radiochemical purities of all HPLC purified tracers were examined with analytical HPLC and were always found to be $\geq 95\%$. The products were stable for up to 4 h in their formulation.

The average radiochemical yield for $[^{18}\text{F}]7\text{-FEHTP}$ (indirect approach) was 8% ($n = 5$) with specific activities in the range of 42–68 GBq/ μmol and an average synthesis time of 75 min from end of bombardment (EOB). For $[^{18}\text{F}]4\text{-FEHTP}$ and $[^{18}\text{F}]6\text{-FEHTP}$, the average radiochemical yield (direct approach) was 18% ($n = 8$) and 13% ($n = 4$), respectively, with specific activities in the range of 70–90 GBq/ μmol and 45–66 GBq/ μmol and an average synthesis time of 90 min since EOB.

Small Animal PET with Xenograft-Bearing Mice. Pilot dynamic PET scans with NMRI nude mice showed accumulation of $[^{18}\text{F}]4\text{-FEHTP}$, $[^{18}\text{F}]6\text{-FEHTP}$, and $[^{18}\text{F}]7\text{-FEHTP}$ in NCI-H69 xenografts. The uptake ratios between xenograft and reference region for all radiotracers were highest between 60 and 75 min p.i. Ratios were higher in scans starting at 60 min post injection than in scans starting immediately after injection. Figure 4 shows the corresponding PET images superimposed on CT images. For a head-to-head comparison, the same animal was scanned with $[^{18}\text{F}]4\text{-FEHTP}$, $[^{18}\text{F}]6\text{-FEHTP}$, and $[^{18}\text{F}]L\text{-FET}$ (Figure 4A, 4B, 4D, respectively). Faint accumulation of radioactivity in bone was observed after $[^{18}\text{F}]6\text{-FEHTP}$ application (Figure 4B). Xenograft accumulation of $[^{18}\text{F}]4\text{-FEHTP}$, $[^{18}\text{F}]6\text{-FEHTP}$, and $[^{18}\text{F}]7\text{-FEHTP}$

were in a similar range and between SUV 0.7 to 1.1 (Figure 5A). $[^{18}\text{F}]L\text{-FET}$ showed the highest uptake value of 1.7 ± 0.16 compared to the three investigated radiotracers ($P < 0.001$). However, all three ^{18}F -labeled tryptophan analogues showed significantly lower background radioactivity than $[^{18}\text{F}]L\text{-FET}$ ($P < 0.005$). SUV ratios between xenograft and background for $[^{18}\text{F}]4\text{-FEHTP}$, $[^{18}\text{F}]7\text{-FEHTP}$, and $[^{18}\text{F}]L\text{-FET}$ ranged from 1.9 to 2.1 (Figure 5B). $[^{18}\text{F}]6\text{-FEHTP}$, showed the highest xenograft to reference ratio of 2.6 ± 0.2 with significance ($P < 0.001$). Compared to the previously published $[^{18}\text{F}]L\text{-FEHTP}$, with a SUV ratio < 2 , the $[^{18}\text{F}]6\text{-FEHTP}$ analogue revealed the best xenograft-to-reference ratio of all possible aromatic-ring substituted $[^{18}\text{F}]$ fluoroethoxy tryptophans.

Stereochemistry configuration is known to affect the transport of many radiolabeled amino acids. We have recently discussed the influence of the stereochemical configuration of amino acid derivatives on PET imaging results.²¹ In general, the LAT system mainly recognizes L-amino acids, although it has been shown that it also transports certain D-amino acids with high affinity such as D-phenylalanine, D-leucine and D-methionine but not D-tryptophan.¹³ In this respect, we cannot exclude that for our new tryptophan analogues, transport kinetics, and/or tumor uptake may differ significantly between the two isomers. In this study, we compared racemic mixtures of the new tracers with enantiomerically pure $[^{18}\text{F}]L\text{-FET}$ and were pleased to note that $[^{18}\text{F}]6\text{-FEHTP}$ outperforms $[^{18}\text{F}]L\text{-FET}$. It is possible that an enantiomerically pure isomer of $[^{18}\text{F}]6\text{-FEHTP}$ (most probably the L-isomer) could perform even better in vivo, especially if the D-isomer in racemic $[^{18}\text{F}]6\text{-$

FEHTP shows significant unfavorable transport and uptake properties.

Ex Vivo Metabolite Studies. In order to assess whether any biotransformation step is involved in the relatively high tumor uptake of [¹⁸F]6-FEHTP, we investigated its in vivo metabolism in the NCI-H69 tumor-bearing mouse. Only intact compound was detected in the plasma, tumor, and urine for this tracer (data not shown) at 60 min p.i. On the basis of these results, we excluded a possible involvement of a biotransformation step in tumor accumulation. For comparison, no parent compound was detected in blood 60 min after injection of the AADC substrate [¹⁸F]FDOPA in the same mouse strain.²⁰ Apparently, the presence of a fluoroethoxy side chain on the phenyl part of the indole core or/and the absence of an unmodified hydroxyl group at the 5-position of tryptophan is not tolerated by the AADC enzyme.

In Vitro Cell Uptake and Efflux Studies. Because [¹⁸F]6-FEHTP showed the best in vivo performance, we wanted to investigate further the mechanism by which it accumulates in vitro in NCI-H69 tumor cells. Figure 6A–C shows the rapid influx of [¹⁸F]6-FEHTP into NCI-H69 cells at 37 and 4 °C, reaching around 20% of the total added radioactivity per milligram of protein within 5 min. After the fast initial uptake, radioactivity reached a steady state after 20 to 40 min with 20% to 40% uptake per mg protein. Uptake was hardly temperature-dependent and was independent of Na⁺ or S-carbidopa. This excludes a major contribution to uptake by any energy- or Na⁺-dependent transport system or by AADC. The LAT1/2 inhibitor BCH reduced uptake to <2%/mg under all conditions.

In the absence of amino acids, the efflux of [¹⁸F]6-FEHTP was slow compared with the uptake at 37 °C and was negligible at 4 °C (Figure 6D). These findings are in perfect agreement with transport by LAT1, which is upregulated in most tumor cells and which is the major transport system for tryptophan analogues. Uptake and efflux characteristics of [¹⁸F]6-FEHTP were similar to those of the previously published analogue and LAT1/2 substrate [¹⁸F]_L-FEHTP.²⁰

CONCLUSIONS

From all four aromatic-ring substituted fluoroethoxy tryptophan analogues (positions 4-, 5-, 6-, and 7-) and compared to [¹⁸F]_L-FET, [¹⁸F]6-FEHTP exhibits the highest tumor-to-background ratio in a small cell lung cancer xenograft model. This gives proof that the positioning of the ¹⁸F-bearing side chain on the indole core has some effect on the in vivo performance of the tryptophan tracer, although these changes are not dramatic. Uptake of [¹⁸F]6-FEHTP seems to take place exclusively via LAT transport with no evidence of in vivo metabolism participating in accumulation. [¹⁸F]6-FEHTP can be considered as another interesting PET probe for imaging LAT activity of tumors.

ASSOCIATED CONTENT

Supporting Information

Detailed synthetic methods and characterization for all intermediates. This material is available free of charge via the Internet at <http://pubs.acs.org>.

AUTHOR INFORMATION

Corresponding Author

*E-mail: simon.ametamey@pharma.ethz.ch. Fax: +41 44 633 13 67. Tel.: +41 44 633 74 63.

Notes

The authors declare no competing financial interest.

ABBREVIATIONS

AADC, aromatic amino acid decarboxylase; APUD, amine precursor uptake and decarboxylation; BCH, 2-amino-2-norbornanecarboxylic acid; [¹¹C]SHTP, 5-hydroxy-L-[β -¹¹C]-tryptophan; EBSS, Earle balanced salt solution; [¹⁸F]4-FEHTP, (4-(2-[¹⁸F]fluoroethoxy)-DL-tryptophan; [¹⁸F]6-FEHTP, (6-(2-[¹⁸F]fluoroethoxy)-DL-tryptophan; [¹⁸F]7-FEHTP, (7-(2-[¹⁸F]fluoroethoxy)-DL-tryptophan; [¹⁸F]2-FPTRP, 2-(3-[¹⁸F]fluoropropyl)-DL-tryptophan); [¹⁸F]5-FPTRP, 5-(3-[¹⁸F]uoropropyl)-DL-tryptophan; [¹⁸F]FACBC, anti-1-amino-3-[¹⁸F]-fluoro-cyclobutane-1-carboxylic acid; [¹⁸F]FAMT, (L-[3-[¹⁸F]-amino-tyrosine; [¹⁸F]FEP, (L-p-(2-[¹⁸F]fluoroethyl)-phenylalanine; [¹⁸F]FDG, 2-deoxy-2-(¹⁸F)fluoro-D-glucose; [¹⁸F]FDOPA, L-3,4-dihydroxy-6-[¹⁸F]fluorophenylalanine; [¹⁸F]_L-FET, O-(2-[¹⁸F]fluoroethyl)-L-tyrosine; [¹⁸F]_L-FEHTP, 5-(2-[¹⁸F]fluoroethoxy)-L-tryptophan; [¹⁸F]FPHCys, methionine (S-(3-[¹⁸F]fluoropropyl)-D-homocysteine; LAT, large amino acid transporter; PET, positron emission tomography; SUV, standardized uptake values; TBAHCO₃, tetrabutylammonium bicarbonate; TBAOH, tetrabutylammonium hydroxide

REFERENCES

- (1) Hanahan, D.; Weinberg, R. A. Hallmarks of cancer: the next generation. *Cell* **2011**, *144* (5), 646–674.
- (2) Youland, R. S.; Kitange, G. J.; Peterson, T. E.; Pafundi, D. H.; Ramiscal, J. A.; Pokorny, J. L.; Giannini, C.; Laack, N. N.; Parney, I. F.; Lowe, V. J.; Brinkmann, D. H.; Sarkaria, J. N. The role of LAT1 in (¹⁸F)-DOPA uptake in malignant gliomas. *J. Neuro-Oncol.* **2013**, *111* (1), 11–18.
- (3) Ganapathy, V.; Thangaraju, M.; Prasad, P. D. Nutrient transporters in cancer: Relevance to Warburg hypothesis and beyond. *Pharmacol. Ther.* **2009**, *121* (1), 29–40.
- (4) McConathy, J.; Yu, W. P.; Jarkas, N.; Seo, W.; Schuster, D. M.; Goodman, M. M. Radiohalogenated nonnatural amino acids as PET and SPECT tumor imaging agents. *Med. Res. Rev.* **2012**, *32* (4), 868–905.
- (5) Schoder, H.; Larson, S. M. Positron emission tomography for prostate, bladder, and renal cancer. *Semin. Nucl. Med.* **2004**, *34* (4), 274–292.
- (6) Sundin, A.; Garske, U.; Orlefors, H. Nuclear imaging of neuroendocrine tumours. *Best. Pract. Res. Clin. Endocrinol. Metab.* **2007**, *21* (1), 69–85.
- (7) Nakanishi, T.; Tamai, I. Solute Carrier Transporters as Targets for Drug Delivery and Pharmacological Intervention for Chemotherapy. *J. Pharm. Sci.* **2011**, *100* (9), 3731–3750.
- (8) Palacin, M.; Estevez, R.; Bertran, J.; Zorzano, A. Molecular biology of mammalian plasma membrane amino acid transporters. *Physiol. Rev.* **1998**, *78* (4), 969–1054.
- (9) Fuchs, B. C.; Bode, B. P. Amino acid transporters ASCT2 and LAT1 in cancer: Partners in crime? *Semin. Cancer Biol.* **2005**, *15* (4), 254–266.
- (10) Gupta, N.; Miyauchi, S.; Martindale, R. G.; Herdman, A. V.; Podolsky, R.; Miyake, K.; Mager, S.; Prasad, P. D.; Ganapathy, M. E.; Ganapathy, V. Upregulation of the amino acid transporter ATB(0,+) (SLC6A14) in colorectal cancer and metastasis in humans. *Biochim. Biophys. Acta, Mol. Basis Dis.* **2005**, *1741* (1–2), 215–223.
- (11) Gupta, N.; Prasad, P. D.; Ghamande, S.; Moore-Martin, P.; Herdman, A. V.; Martindale, R. G.; Podolsky, R.; Mager, S.; Ganapathy, M. E.; Ganapathy, V. Up-regulation of the amino acid transporter ATB(0,+) (SLC6A14) in carcinoma of the cervix. *Gynecol. Oncol.* **2006**, *100* (1), 8–13.
- (12) Karunakaran, S.; Ramachandran, S.; Coothankandaswamy, V.; Elangovan, S.; Babu, E.; Periyasamy-Thandavan, S.; Gurav, A.;

- Gnanaprakasam, J. P.; Singh, N.; Schoenlein, P. V.; Prasad, P. D.; Thangaraju, M.; Ganapathy, V. SLC6A14 (ATB(0+)) Protein, a Highly Concentrative and Broad Specific Amino Acid Transporter, Is a Novel and Effective Drug Target for Treatment of Estrogen Receptor-positive Breast Cancer. *J. Biol. Chem.* **2011**, *286* (36), 31830–31838.
- (13) Yanagida, O.; Kanai, Y.; Chairoungdua, A.; Kim, D. K.; Segawa, H.; Nii, T.; Cha, S. H.; Matsuo, H.; Fukushima, J.; Fukasawa, Y.; Tani, Y.; Taketani, Y.; Uchino, H.; Kim, J. Y.; Inatomi, J.; Okayasu, I.; Miyamoto, K.; Takeda, E.; Goya, T.; Endou, H. Human L-type amino acid transporter 1 (LAT1): characterization of function and expression in tumor cell lines. *Biochim. Biophys. Acta, Biomembr.* **2001**, *1514* (2), 291–302.
- (14) Fotiadis, D.; Kanai, Y.; Palacin, M. The SLC3 and SLC7 families of amino acid transporters. *Mol. Aspects. Med.* **2013**, *34* (2–3), 139–158.
- (15) Kaira, K.; Oriuchi, N.; Takahashi, T.; Nakagawa, K.; Ohde, Y.; Okumura, T.; Murakami, H.; Shukuya, T.; Kenmotsu, H.; Naito, T.; Kanai, Y.; Endo, M.; Kondo, H.; Nakajima, T.; Yamamoto, N. LAT1 expression is closely associated with hypoxic markers and mTOR in resected non-small cell lung cancer. *Am. J. Transl. Res.* **2011**, *3* (5), 468-U104.
- (16) Wiriyasermkul, P.; Nagamori, S.; Tominaga, H.; Oriuchi, N.; Kaira, K.; Nakao, H.; Kitashoji, T.; Ohgaki, R.; Tanaka, H.; Endou, H.; Endo, K.; Sakurai, H.; Kanai, Y. Transport of 3-Fluoro-L- α -Methyl-Tyrosine by Tumor-Upregulated L-Type Amino Acid Transporter 1: A Cause of the Tumor Uptake in PET. *J. Nucl. Med.* **2012**, *53* (8), 1253–1261.
- (17) Bourdier, T.; Shepherd, R.; Berghofer, P.; Jackson, T.; Fookes, C. J. R.; Denoyer, D.; Dorow, D. S.; Greguric, I.; Gregoire, M. C.; Hicks, R.; Katsifis, A. Radiosynthesis and Biological Evaluation of L- and D-S-(3-[F-18]Fluoropropyl)homocysteine for Tumor Imaging Using Positron Emission Tomography. *J. Med. Chem.* **2011**, *54* (6), 1860–1870.
- (18) Wang, L. M.; Lieberman, B. P.; Plossl, K.; Qu, W. C.; Kung, H. F. Synthesis and comparative biological evaluation of L- and D-isomers of F-18-labeled fluoroalkyl phenylalanine derivatives as tumor imaging agents. *Nucl. Med. Biol.* **2011**, *38* (3), 301–312.
- (19) Martarello, L.; McConathy, J.; Camp, V. M.; Malveaux, E. J.; Simpson, N. E.; Simpson, C. P.; Olson, J. J.; Bowers, G. D.; Goodman, M. M. Synthesis of syn- and anti-1-amino-3-[F-18]fluoromethylcyclobutane-1-carboxylic acid (FMACBC), potential PET ligands for tumor detection. *J. Med. Chem.* **2002**, *45* (11), 2250–2259.
- (20) Kramer, S. D.; Mu, L.; Muller, A.; Keller, C.; Kuznetsova, O. F.; Schweinsberg, C.; Franck, D.; Muller, C.; Ross, T. L.; Schibli, R.; Ametamey, S. M. 5-(2-¹⁸F-fluoroethoxy)-L-tryptophan as a substrate of system L transport for tumor imaging by PET. *J. Nucl. Med.* **2012**, *53* (3), 434–442.
- (21) Chiotellis, A.; Mu, L.; Muller, A.; Selivanova, S. V.; Keller, C.; Schibli, R.; Kramer, S. D.; Ametamey, S. M. Synthesis and biological evaluation of (1)(8)F-labeled fluoropropyl tryptophan analogs as potential PET probes for tumor imaging. *Eur. J. Med. Chem.* **2013**, *70*, 768–780.
- (22) Lovenberg, W.; Weissbach, H.; Udenfriend, S. Aromatic L-Amino Acid Decarboxylase. *J. Biol. Chem.* **1962**, *237* (1), 89–93.
- (23) Koopmans, K. P.; Neels, O. N.; Kema, I. P.; Elsinga, P. H.; Links, T. P.; de Vries, E. G. E.; Jager, P. L. Molecular imaging in neuroendocrine tumors: Molecular uptake mechanisms and clinical results. *Crit. Rev. Oncol. Hemat.* **2009**, *71* (3), 199–213.
- (24) Sundin, A.; Eriksson, B.; Bergstrom, M.; Langstrom, B.; Oberg, K.; Orlefors, H. PET in the diagnosis of neuroendocrine tumors. *Ann. N. Y. Acad. Sci.* **2004**, *1014*, 246–257.
- (25) Vachtenheim, J.; Novotna, H. Expression of the aromatic L-amino acid decarboxylase mRNA in human tumour cell lines of neuroendocrine and neuroectodermal origin. *Eur. J. Cancer* **1997**, *33* (14), 2411–2417.
- (26) Pearse, A. G. E. APUD – Concept, Tumors, Molecular Markers and Amyloid. *Mikroskopie* **1980**, *36* (9–10), 257–269.
- (27) Lu, M. Y.; Liu, Y. L.; Chang, H. H.; Jou, S. T.; Yang, Y. L.; Lin, K. H.; Lin, D. T.; Lee, Y. L.; Lee, H.; Wu, P. Y.; Luo, T. Y.; Shen, L. H.; Huang, S. F.; Liao, Y. F.; Hsu, W. M.; Tzen, K. Y. Characterization of Neuroblastic Tumors Using F-18-FDOPA PET. *J. Nucl. Med.* **2013**, *54* (1), 42–49.
- (28) Neels, O. C.; Koopmans, K. P.; Jager, P. L.; Vercauteran, L.; van Waarde, A.; Doorduin, J.; Timmer-Bosscha, H.; Brouwers, A. H.; de Vries, E. G. E.; Dierckx, R. A. J. O.; Kema, I. P.; Elsinga, P. H. Manipulation of [C-11]-5-hydroxytryptophan and 6-[F-18]fluoro-3,4-dihydroxy-L-phenylalanine accumulation in neuroendocrine tumor cells. *Cancer Res.* **2008**, *68* (17), 7183–7190.
- (29) Miko, E.; Margitai, Z.; Czimerer, Z.; Varkonyi, I.; Balazs, D.; Lanyi, A.; Bacso, Z.; Scholtz, B. miR-126 inhibits proliferation of small cell lung cancer cells by targeting SLC7AS. *FEBS Lett.* **2011**, *585* (8), 1191–1196.
- (30) Carney, D. N.; Gazdar, A. F.; Bepler, G.; Guccion, J. G.; Marangos, P. J.; Moody, T. W.; Zweig, M. H.; Minna, J. D. Establishment and Identification of Small Cell Lung-Cancer Cell-Lines Having Classic and Variant Features. *Cancer Res.* **1985**, *45* (6), 2913–2923.
- (31) Damont, A.; Hinnen, F.; Kuhnast, B.; Schollhorn-Peyronneau, M. A.; James, M.; Luus, C.; Tavitian, B.; Kassiou, M.; Dolle, F. Radiosynthesis of [(18)F]DPA-714, a selective radioligand for imaging the translocator protein (18 kDa) with PET. *J. Labelled Compd. Radiopharm.* **2008**, *51* (7–8), 286–292.
- (32) Darmanin, T.; Guitard, F. One-pot method for build-up nanoporous super oil-repellent films. *J. Colloid Interface Sci.* **2009**, *335* (1), 146–149.
- (33) Qu, W. C.; Kung, M. P.; Hou, C.; Benedum, T. E.; Kung, H. F. Novel styrylpyridines as probes for SPECT imaging of amyloid plaques. *J. Med. Chem.* **2007**, *50* (9), 2157–2165.
- (34) Anantharamaiah, G. M.; Sivanandaiah, K. M. Transfer Hydrogenation – Convenient Method for Removal of Some Commonly Used Protecting Groups in Peptide-Synthesis. *J. Chem. Soc., Perkin Trans. 1* **1977**, No. 5, 490–491.
- (35) Atherton, E.; Bury, C.; Sheppard, R. C.; Williams, B. J. Stability of Fluorenylmethoxycarbonylaminos in Peptide-Synthesis – Cleavage by Hydrogenolysis and by Dipolar Aprotic-Solvents. *Tetrahedron Lett.* **1979**, No. 32, 3041–3042.
- (36) Felix, A. M.; Heimer, E. P.; Lambros, T. J.; Tzougraki, C.; Meienhofer, J. Rapid Removal of Protecting Groups from Peptides by Catalytic Transfer Hydrogenation with 1,4-Cyclohexadiene. *J. Org. Chem.* **1978**, *43* (21), 4194–4196.